Nanoscale Surface Lamellar Orientation and Lamellar Doubling in Ultrathin UHMW−PE Films

Thomas Keller, Matthias Grosch, and Klaus D. Jandt*

Institute of Materials Science & Technology (IMT), Chair in Materials Science, Friedrich-Schiller-University Jena, Löbdergraben 32, D-07743 Jena, Germany

Received March 13, 2007; Revised Manuscript Received May 2, 2007

ABSTRACT: Nanostructured, highly oriented, ultrathin ultrahigh-molecular weight polyethylene (UHMW−PE) films have been generated by melt drawing at temperatures in proximity to the mean polymer melting point (142.3 ± 0.2 °C, as determined by differential scanning calorimetry). In this temperature regime, the crystal nuclei size, the rheology, and the mobility of melted polymer chains strongly depend on the polymer temperature and therefore affect the development of the crystal morphology of the film. By stepwise increasing of the polymer processing temperature from 138 to 146 °C in steps of 2 °C, the mean lamellar thickness increases from 25 ± 2 to 32 ± 5 nm, as observed with tapping mode atomic force microscopy (AFM). Parallel with increasing thickness, the lamellae arrangement in the drawn films change from staggered to stacked and uncoordinated. On the basis of this observed surface crystal morphology, a model is proposed describing the temperature-dependent evolution of the lamellar arrangement in the melt drawn films. In sufficiently thin films, i.e., thickness of the order of a lamellar width (≈100 nm), discrete lamellae thickness values of 16 ± 2, 29 ± 2, and 62 ± 2 nm are observed in the UHMW−PE film drawn at a temperature of 140 °C, indicating the onset of lamellar doubling. For the first time, indications for a mechanical strain-induced lamellar doubling during film drawing are reported.

Introduction

Ultrahigh molecular weight polyethylene (UHMW−PE) is a technologically relevant polymer used, e.g., in high tensile strength fibers[1] or biomaterials, such as endoprosthesis.[2,3] For advanced applications, such as in the biomedical field, it is desirable to optimize UHMW−PE surface properties down to the nanometer scale, as this may control frictional properties or the biological performance of the material.[4] Such modifications comprise an adjustment of topographic surface features on the micro- and nanoscales as well as the surface chemistry.[5]

The generation of nanostructured, highly oriented semicrystalline ultrathin polymer films by melt drawing was demonstrated by Petermann and Gohil.[6] Melt drawing techniques have been applied to various polymers to obtain highly oriented, semicrystalline and easy-to-handle films that may be investigated by transmission electron microscopy (TEM) without further preparation steps like thinning. In thermoplastic polymers, crystal morphologies like a needle-crystal structure (shish) were observed for example in polypropylene (PP),[7] polybutene-1 (PB1),[8,9] and isotactic polystyrene (PS)[10] films by atomic force microscopy (AFM). In high-density polyethylene (HD−PE)[11] melt drawn films, the typical morphology are lamellar crystals (kebab). Such crystals often protrude from the film surface and therefore generate topographic steps of a 0.5−4 nm height,[12] as shown by AFM.

Zhao et al. reported a TEM study on melt drawn UHMW−PE/HD−PE blend thin films.[13] Such blends exhibit both, a lamellar (as in pure HD−PE) and a needle crystal morphology. The number of needle crystals increases with increasing UHMW−PE content of the blend to an almost complete needle crystal morphology at 80 wt % UHMW−PE.[13] Although from this one would expect a well-defined needle crystal morphology in pure UHMW−PE films, no distinct development of either a lamellar or a needle crystal morphology was achieved, which was attributed to serious entanglements in the pure UHMW−PE.[13]

In the current study, it is demonstrated that for ultrathin UHMW−PE films a variety of lamellar crystallite sizes and lateral arrangements can be accomplished at the film surface.

The choice of polymer temperature for melt drawing was inspired by previous work of Rastogi et al. on UHMW−PE chain mobility in the intermediate temperature regime between solid and melt.[14]

To the best knowledge of the authors, there is no systematic study so far that shows the development of exclusive lamellar crystal film morphologies of pure ultrathin UHMW−PE film surfaces. It is demonstrated that relatively small variations in the temperature of the UHMW−PE melt within an intermediate temperature regime significantly influence the crystal morphology in the film, thus allowing to tailor the surface morphology of the UHMW−PE ultrathin films. The variations of observed film morphologies are explained by a simple model involving the temperature dependence of the solid−liquid phase transition. For extremely thin UHMW−PE films, lamellar doubling was observed.

Experimental Section

Commercially available UHMW−PE powder (Sigma Aldrich, Schnelldorf, Germany, average molecular weight $M_w = 3 \times 10^6 - 6 \times 10^6$ g/mol, and density ρ (298 K) = 0.94 g/cm^3) and xylene as solvent (synthesis grade, Merck KGaA, Darmstadt, Germany) were used.

The UHMW−PE powder was dissolved in xylene to obtain a 0.5 wt % polymer solution. Subsequently, a few droplets of this solution were given onto a heated glass-plate. The latter was fixed on top of a precision heating plate that was kept at temperatures between 136−146 °C, as measured by a calibrated thermocouple. After evaporation of the solvent and equilibration to the final drawing temperature (approximately 30 s), a thin polymer film was manually drawn from the resulting polymer melt reservoir by tweezers at a drawing rate of approximately 1 cm/s and fixed on

* Corresponding author. Telephone: +49 3641 947730. Fax: +49 3641 947732. E-mail: k.jandt@uni-jena.de.

10.1021/ma070613x CCC: $37.00
Published on Web 07/06/2007

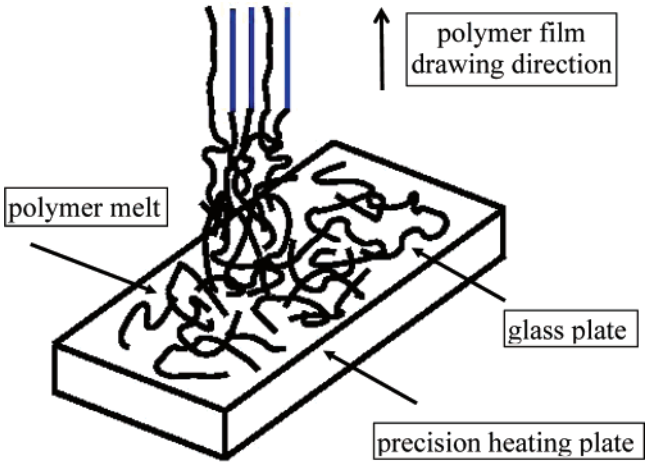

Figure 1. Sketch of the drawing process. The UHMW−PE is drawn from the melt. The orientation of the molecules during the drawing process enhances crystallization. The drawing direction is vertical.

freshly cleaved mica (standard quality, Plano GmbH, Wetzlar, Germany) or glass microscope slides. Figure 1 shows a sketch of the polymer thin film preparation.

Differential scanning calorimetry (DSC) of the native UHMW−PE powder was performed under nitrogen atmosphere with a NETZSCH DSC 204 F1 instrument (NETZSCH GmbH, Selb, Germany). An Indium standard was used for calibration of the DSC. For the DSC measurement, the powder was placed in an aluminum pan. Each sample was heated from room temperature to 180 °C at a rate of 10 °C/min, kept for 5 min at 180 °C, cooled to room temperature at a rate of 10 °C/min, and again heated at 10 °C/min to 180 °C. The heat transfer to or from the sample was recorded. The sample mass was varied as 19.1, 9.1, and 5.3 mg to take into account the thermal lag that affects the polymer melting temperature through a sample mass dependence.[15]

Tapping mode scanning force microscopy images were recorded using a Dimension 3100 AFM (Digital Instruments, Veeco, CA, USA) with a Nanoscope IV Controller. Topographic, amplitude and phase images were recorded simultaneously in tapping mode at ambient temperature in air with an etched silicon probe on a rectangular-shaped cantilever (125 μm × 35 μm) (RTESP, Digital Instruments) with an approximate resonance frequency of 300 kHz and a spring constant of 40 N/m. To avoid sample damage, measurements were performed after adjusting the amplitude set-point just before loss of contact to the surface. The scan rate was 2 μm/s. Tapping mode phase imaging is especially suited for the analysis of semicrystalline polymer surfaces since this technique offers the possibility to distinguish chemically identical crystalline from amorphous regions by their different elastic behavior which is probed by the tip and reflected in a phase shift.[16] A first-order flattening function was applied to take into account a macroscopic sample tilt.

TEM samples were prepared from the polymer film deposited on the microscope slides. The film was cut into small pieces, lifted from the glass in deionized H_2O, fished on a Cu− TEM grid (mesh 400) and finally fixed to the TEM grid by putting the grid onto a soaking filter paper. Subsequently, the polymer film was stained by a droplet of an aqueous phosphotungstic acid solution (obtained as hydrate from Alfa Aesar, Karlsruhe, Germany) that was diluted to a 0.5 wt % solution with demineralized H_2O. Then, the film was washed with demineralized H_2O and left to dry in vacuum at 40 °C overnight. The contrast of the TEM micrographs originates from a preferential diffusion of the phosphotungstic acid into the less dense, amorphous regions of the sample. Because of the higher absorption cross section of tungsten, the amorphous regions appear darker when imaged by electron microscopy in transmission. TEM and electron beam diffraction (EBD) analysis were performed on a JEOL 3010 instrument operated at 300 kV.

Results and Discussion

Thermal Analysis. Calorimetric DSC measurements of the powder starting material were performed to determine the polymer melting range and therefore suitable temperatures for the film drawing. The peak temperatures of minimum or maximum heat flux to or from the sample are considered to be a measure of the mean melting and crystallization temperatures,[15] respectively, which for convenience in the following

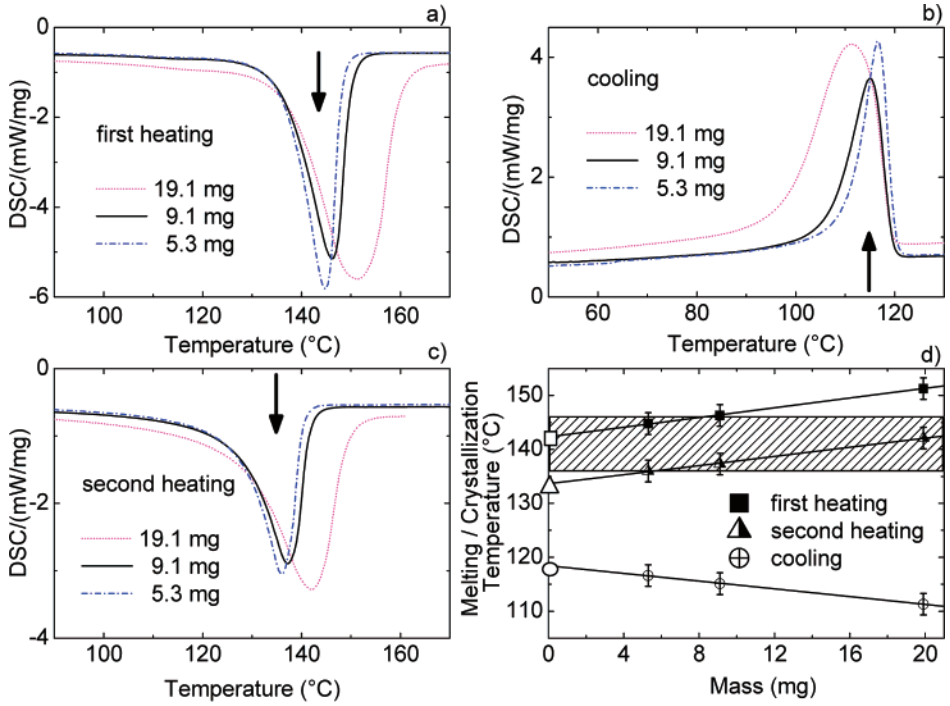

Figure 2. DSC curves of the UHMW−PE powder for sample masses as indicated in the insets. Key: (a) first heating curve with melting (arrow); (b) cooling with crystallization (arrow); (c) second heating with remelting (arrow); (d) mass dependence of mean melting and crystallization points and linearly extrapolated to zero mass [(□) 142.3 ± 0.2, (△) 133.6 ± 0.3, and (○) 118.5 ± 0.1 °C]. The shaded area indicates the temperatures of film preparation.

Table 1. Peak DSC Melting and Crystallization Temperatures of the UHMW−PE Powder for Different Sample Masses[a]

	temperatures (°C)		
sample mass (mg)	first heating	cooling	second heating
19.1	151.3 ± 0.1	111.3 ± 0.1	142.1 ± 0.1
9.1	146.3 ± 0.1	115.1 ± 0.1	137.3 ± 0.1
5.3	144.8 ± 0.1	116.6 ± 0.1	136.0 ± 0.1
0	142.3 ± 0.2[b]	118.5 ± 0.1[b]	133.6 ± 0.3[b]

[a] The errors are standard deviations of Gaussian fits. [b] Extrapolated.

will be referred to as polymer melting/crystallization point. Figure 2 a, b, and c show the heating, cooling and second heating curves in the melting and crystallization ranges of the UHMW−PE for the different sample masses. Peak melting and crystallization temperatures are given in Table 1. With decreasing sample mass, the thermal lag is reduced[15] as can be seen from the shift of the melting peak toward lower temperature and the crystallization toward higher temperature, respectively. In Figure 2d, the obtained melting and crystallization temperatures are linearly extrapolated to zero sample-mass, and the resulting values are 142.3 ± 0.2 and 133.6 ± 0.3 °C for the first and the following heating of the UHMW−PE powder, respectively, whereas crystallization occurs at 118.5 ± 0.1 °C. The shaded area in Figure 2 d indicates the temperature range used for the film drawing. A shift in melting temperature is known from literature from first to second heating, since the melting temperature depends on the mean crystallite size in the polymer.[17] The onset and end of the melting and crystallization peak define the melt and crystallization temperature range of the sample, respectively. Extrapolated to zero mass, for the first heating the melting range of the polymer is 135.7−142.3 °C, for the cooling the range of crystallization is 114.4−118.5 °C, and for the following heating the melting range is 127.6−133.6 °C.

Drawing Conditions. The UHMW−PE was dissolved in xylene as described in the Experimental Section. For dissolving the UHMW−PE, the solvent was heated to a temperature of 110 °C. During the solution process, the UHMW−PE powder first agglomerated and started to swell. Single polymer chains got dissolved and increased the viscosity of the solvent. The swollen polymer transformed to a gel network.[18] At a sufficiently long time of stirring the gel network more and more disentangled due to the applied shear forces during stirring. Finally, only a negligible fraction of the polymer chains remained in a swollen state with entanglement-restricted mobility. After this polymer solution was transferred onto the hot glass-plate and subsequent evaporation of the solvent, the ultrathin films were drawn.

To the best knowledge of the authors, thin film and crystallization properties of UHMW−PE are not yet documented in detail up to now. Jian et al. investigated the dependence of UHMW−PE fiber quality on rheological properties.[19] It was found that fiber drawability is ensured with an appropriate viscosity. If the viscosity is too high, single molecules are hindered in the orientation along the drawing direction and therefore, the drawability is low. On the other hand, for a too small viscosity, the macromolecules disentangle quickly and are drawn out of the melt as isolated fibers. Besides the temperature, the viscosity is to a large extent determined by the polymer concentration and the degree of entanglements in the network, limiting the drawability.

Temperature Dependence of Surface Crystal Morphology. Scanning probe microscopy techniques are the most appropriate methods to study the surface morphology of polymer films up to molecular resolution.[20] Up to now, only scanning tunneling microscopy (STM) has been utilized to investigate the surface

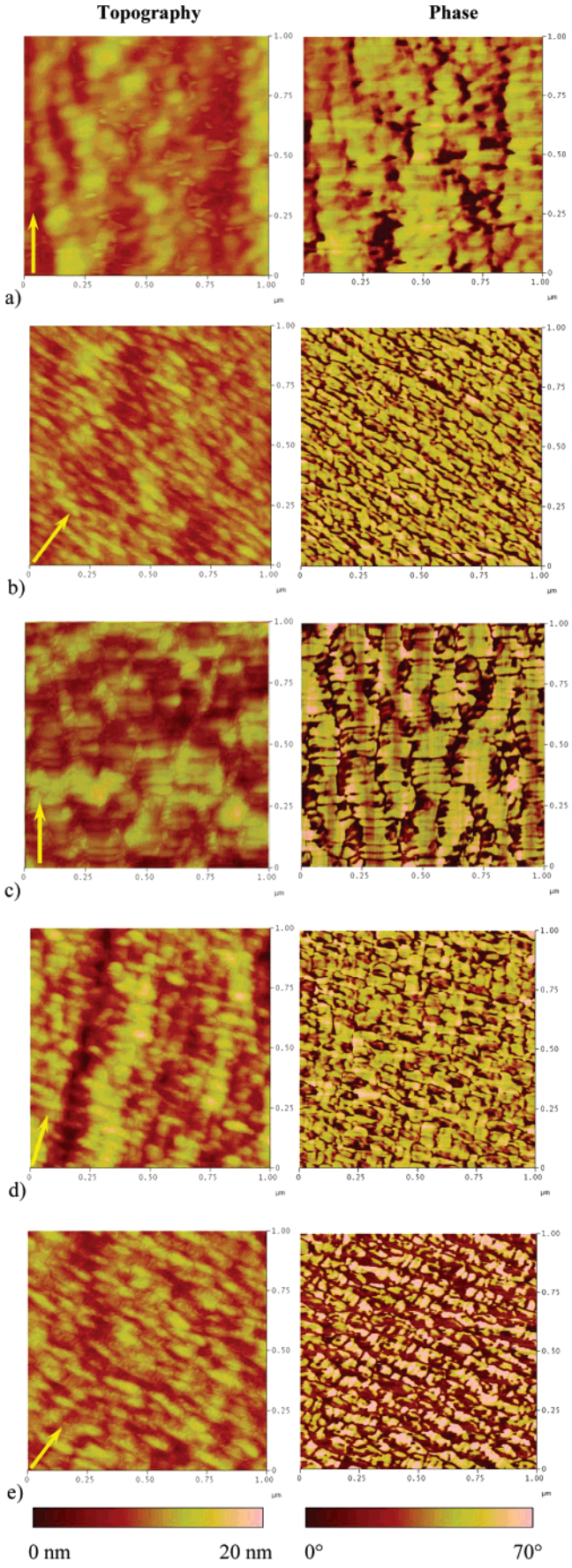

Figure 3. Morphology of films drawn at (a) 136, (b) 138, (c) 140, (d) 142, and (e) 144 °C. The scan size is 1 μm × 1 μm; the color scale corresponds to the topographic (left image) and phase (right image) change of 0−20 nm and 0−70°, respectively. The arrows indicate the drawing direction of the UHMW−PE film.

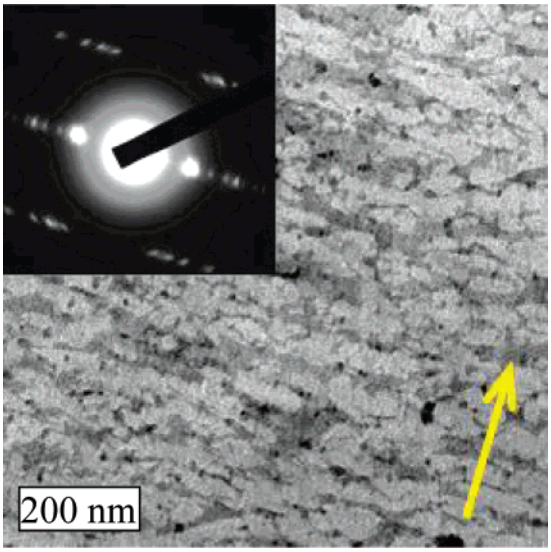

Figure 4. TEM bright field micrograph of the crystalline structure of the UHMW−PE film along with the corresponding EBD pattern in the inset. The film was drawn at a temperature of 138 °C. The film drawing direction is indicated by the arrow and can be identified from the EBD texture. The staggered lamellar morphology of the film is visible.

crystal morphology of an UHMW−PE blend film containing 20 wt % HD−PE,[21] whereas surfaces of pure ultrathin HD−PE have been analyzed by STM[22] and AFM.[11] In the work presented here, the surface crystal morphologies have been examined by AFM tapping mode in order to characterize the surface morphology of the ultrathin UHMW−PE films.

A series of AFM topographic and phase images of UHMW−PE film surfaces drawn at temperatures in proximity to the polymer melting point, i.e., from 136 °C to 144 °C in increasing steps of 2 °C, is shown in Figure 3, parts a−e, respectively. In Figure 3, the brightest regions in the topographic (left) and phase (right) images correspond to height and phase shifts of 20 nm and 70°, respectively. Lateral structures appear more distinct in the phase images, as the phase contrast enhances the elasticity difference between crystalline and amorphous regions. The more rigid crystalline regions will appear bright, as the former will exhibit a strong repulsive force on deformation to the AFM cantilever, whereas in the amorphous rubbery state regions, such repulsive forces will be absent.[16]

At 136 °C (Figure 3a), the polymer is in the low-temperature part of the melt temperature range. This means, that crystallization has already begun in the relaxed melt on the hot glass-plate before the film drawing process started. Prior to drawing, these crystal nuclei presumably do not exhibit a preferred orientation. By mechanical stretching during the film processing the orientation distribution and lamellar size with respect to the drawing direction is induced. The lamellar orientation along the drawing direction as well as the lamellar widths, however, are inhomogeneous, as shown in Figure 3a. An ordered morphology and well-defined lamellae are absent.

The film drawn at 138 °C (Figure 3b) exhibits a significantly finer crystal surface morphology, i.e., the lamellae arrangement is almost entirely staggered.[23,24] The lamellar thickness and width of the films drawn at 138 °C vary less than those of the films drawn at 136 °C and are 25 ± 2 and 154 ± 13 nm, respectively. Such variations within a single lamella may originate from a rearrangement of separate crystals.

In films drawn at 140 °C (Figure 3c) most of the crystal lamellae are aligned in well ordered stacks. The lateral alignment of lamellae to a stacked fiber super-structure with a well-defined lamellar thickness of 26 ± 3 nm and width of 103 ± 12 nm is clearly visible.

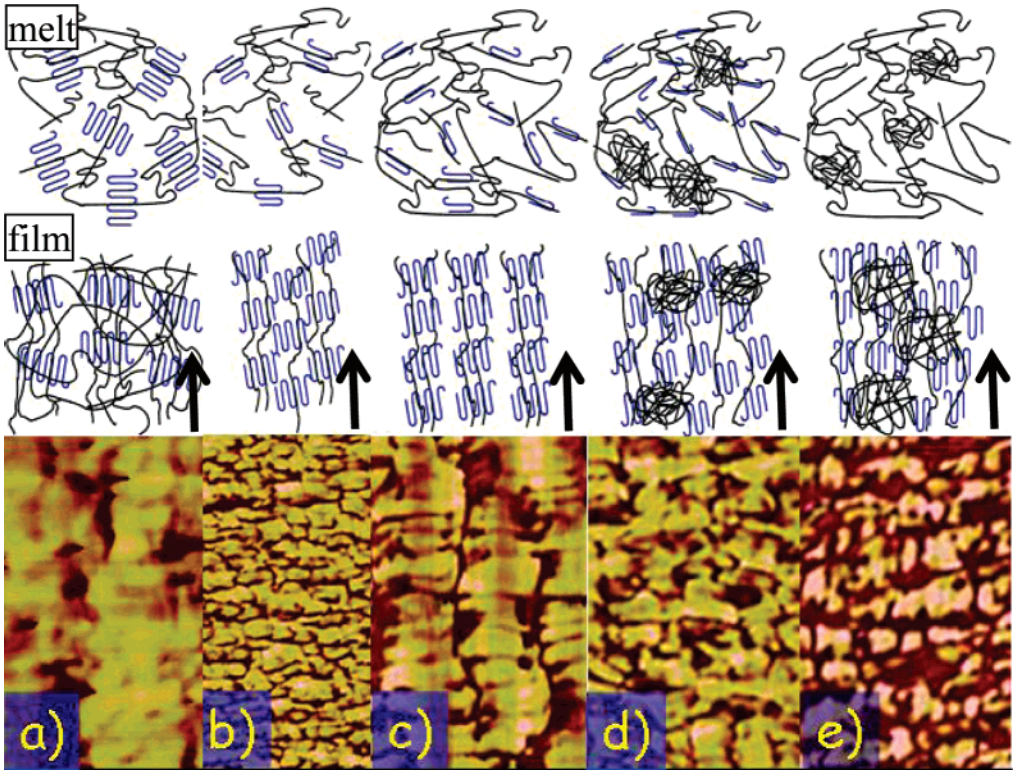

Figure 5. Model for the temperature dependence of the crystal structure development close to the polymer melting point at (a) 136, (b) 138, (c) 140, (d) 142, and (e) 144 °C. Top: crystal arrangement in the melt, middle: surface morphology resulting in the drawn films, bottom: experimentally observed lamellar arrangement (AFM). With increasing temperature, the amount and size of crystals in the melt decreases, leading to higher flexibility of the polymer chains and the remaining crystals. The arrows indicate the drawing direction of the UHMW−PE film.

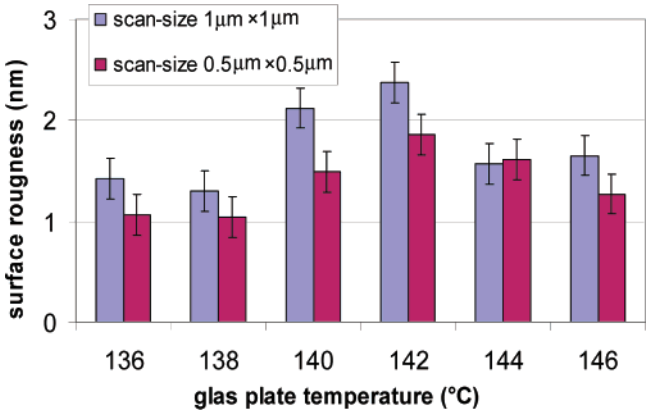

Figure 6. RMS surface roughness for two different image sizes (1 μm × 1 μm and 0.5 μm × 0.5 μm) determined by AFM. The image indicates a roughness maximum near 142 °C in agreement with the maximum of the second DSC melting peak, when the powder structure is lost after the first DSC melting and cooling cycle.

The surface topography of the film drawn at 142 °C (Figure 3d) exhibits individual lamellae with a thickness and width of 31 ± 3 and 102 ± 17 nm, respectively. Compared to the films drawn at 138 and at 140 °C, the structural anisotropy is significantly reduced. Especially in the topographic image (Figure 3d left), the orientational order along the drawing direction is clear, but significantly less distinct than at films drawn at 140 °C.

In films drawn at 144 °C (Figure 3e), predominantly lamellae with a thickness 33 ± 6 nm and width of 98 ± 16 nm are observed at the film surface. The higher regularity of lamellar thickness, width and orientational anisotropy compared to the film drawn at 142 °C indicates that the crystal morphology has been created almost entirely during the film drawing process. The film morphology does therefore not reflect the state of chain or crystal nuclei orientation within the melt, but rather the drawing and cooling conditions.

Table 2. Lateral Lamellar Dimensions and Type of Lamellar Arrangements as a Function of the Polymer Temperature during Film Processing

temp (°C)	lamellar width (nm)	lamellar thickness (nm)	lamellar arrangement
138	154 ± 13	25 ± 2	staggered, laterally shifted
140	103 ± 12	26 ± 3	stacked
142	102 ± 17	31 ± 3	staggered, less anisotropic
144	98 ± 16	33 ± 6	staggered, less anisotropic
146	96 ± 29	32 ± 5	staggered, less anisotropic

The surface morphology of the film drawn at 146 °C is similar to the one drawn at 144 °C, and therefore AFM images are omitted here. Above 144 °C, the principal mechanism of the film drawing process remains the same as the polymer is fully melted. The resulting film crystal morphology is therefore not influenced by increasing the temperature of the polymer melt that only slightly decreases its viscosity.

Table 2 summarizes the mean lamellar thickness and width for the investigated films drawn at glass-plate temperatures between 136−146 °C, obtained from the analysis of the AFM phase images shown in Figure 3a−e. To study the relation between the crystal topography on the film surface and within the bulk, AFM and TEM analysis of the ultrathin UHMW−PE films are compared. An example of a transmission electron micrograph for a film drawn at 138 °C is shown in Figure 4. The less dense amorphous regions appear dark due to the staining agent, which diffuses more quickly as compared to the crystalline lamellae. Comparing to Figure 3b, the TEM investigation confirms the agreement between the surface and bulk crystal morphology.

Model for Temperature-Dependent Crystal Morphology. In the polymer solid/melt coexistence temperature range, polymer crystals or crystal nuclei exist.[25] The crystals incorporated in the partial melt generate stiff entanglements and lead to a dramatic increase in viscosity.[26,27] With increasing tem-

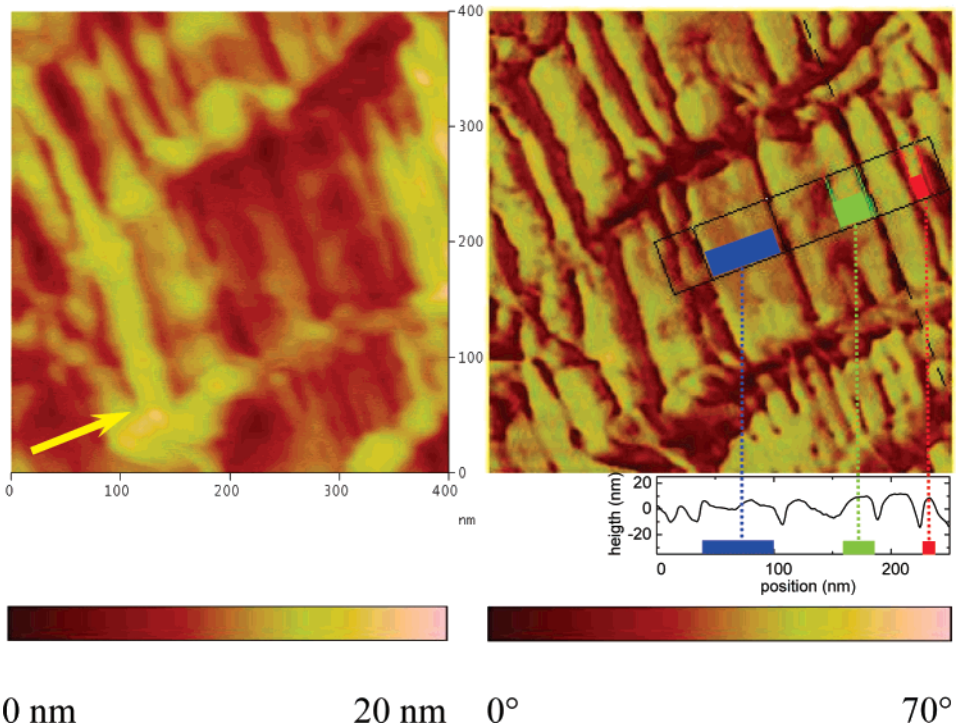

Figure 7. Regular pattern formation in ultrathin films drawn at 140 °C. AFM topographic image (left) and a low-pass filtered phase contrast view (right) with a profile showing distinct lamellae thickness values for the as drawn film at 140 °C. The scan size is 0.4 μm × 0.4 μm, the image color corresponds to the topographic (left) and phase change 0−20 nm and 0−70°, respectively. The arrow indicates the drawing direction of the UHMW−PE film.

perature, the amount of crystals and the mean crystal size in the partial melt decreases. Above a certain temperature, no crystals exist and the polymer is fully melted. Upon further increasing the polymer temperature, the viscosity will further decrease, as a higher molecular mobility leads to a larger intermolecular distance and lower intermolecular forces.

Both, the dramatic variation in viscosity as well as the temperature dependence of the crystal size and amount prior to film drawing is expected to influence the resulting film morphological properties. On the other hand, at a sufficiently high temperature the principal mechanism of film building is not changing with further increasing the polymer temperature.

A sketch of a model for the temperature-dependent development of the crystal morphology is depicted in Figure 5 along with representative AFM micrographs taken from Figure 3. At low glass-plate temperatures used in the current study (136 °C, Figure 5a), relatively large, unoriented crystals exist within the partially melted polymer. During drawing, these crystals align themselves parallel to the drawing direction. The stiff crystals, however, partially inhibit a perfect alignment and orientation during drawing. At higher temperatures (138−142 °C, Figure 5b−d), the amount of crystals and their average size decreases in the melt, associated with more flexibility in alignment during film drawing as well as a higher fraction of newly nucleated crystals in the film. Above the temperature, where all crystals are fully melted (144 °C Figure 5e, 146 °C), the whole crystallization occurs not until the film is drawn from the glass-plate. A strain-induced crystallization during film drawing is likely and explains the highly uniform crystal lamellae alignment.

A transition from a staggered lamellar arrangement at 138 °C (i.e., lamellae showing a lateral shift) and toward a stacked arrangement at 140 °C can be explained by a decrease in melt viscosity with increasing temperature. Crystal entanglements already exist in the melt.[28] On one hand, at 140 °C, the existing lamellar crystals are sufficiently small and seldom in order to permit a flexible crystal and polymer chain alignment along the drawing direction. On the other hand, the aligned crystals serve as nucleation sites to build up the experimentally observed highly ordered stacked crystal morphology.

As shown in Figure 6, the root-mean-square (rms) surface roughness of the melt drawn UHMW−PE films reaches a maximum at a temperature close to the bulk polymer melting point as determined by DSC, which can be explained by a maximal height difference between amorphous areas and well-defined crystalline lamellae.

The highly ordered stacked lamellae obtained at a glass-plate temperature of 140 °C, shown in Figure 3c, are in contrast to the findings of Zhao et al.[13] who report a poor development of either a fibrous (needle) crystal or lamellar structure in thin UHMW−PE films. Zhao et al. argue that the reason for this is a serious entanglement density in the pure UHMW−PE. When UHMW−PE was blended with HD−PE, Zhao et al.[13] report a "smooth transition" from shish-kebab-like fibrous crystals with lamellar overgrowth toward fibrous crystals (extended chain nanofibrils with their fibrous axis aligned parallel to the drawing direction) with increasing UHMW−PE content. However, above 80 wt % UHMW−PE, a high entanglement density and therefore reduced chain mobility in melt or solution disturbs the purely fibrous alignment of extended chains. The lateral growth of lamellae is possibly due to the smaller molecular weight fraction, which is less entangled, more free in orientation and therefore an alignment along single high-molecular weight chains or fibers parallel to the drawing direction is likely. In the current study, the observation of a solely lamellar crystal film morphology is explained by a slightly higher molecular weight of 3×10^6 to 6×10^6 g/mol and a lower drawing speed of 1 cm/s as compared to a molecular weight of 1.5×10^6 g/mol and a drawing speed of 10 cm/s used in the work of Zhao et al.,[13] respectively. Especially the higher drawing speed facilitates the generation of needle crystal structure.[6]

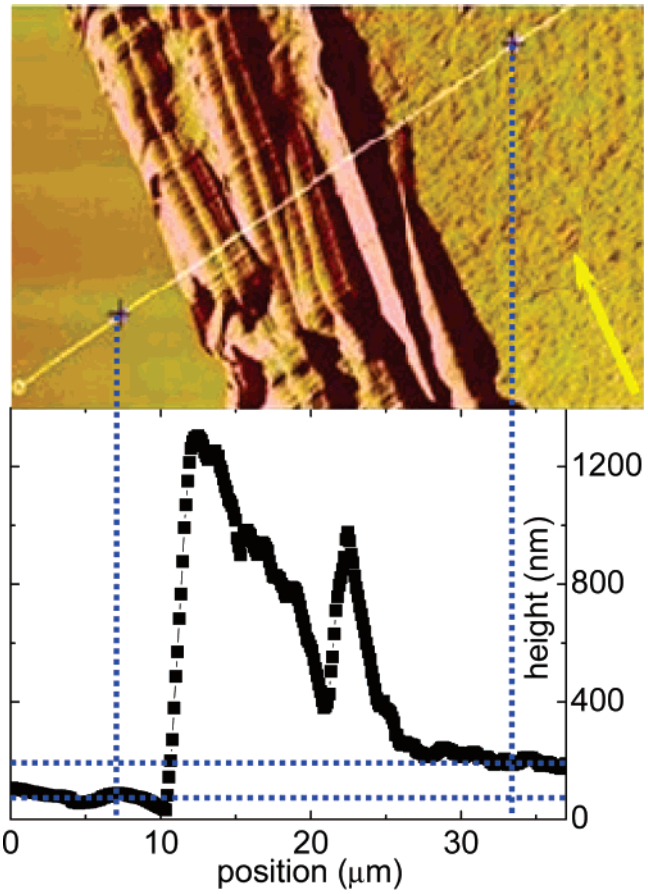

Figure 8. Top: Phase image with a horizontal size of 50 μm and a color range corresponding to a phase change 0−35°. The image shows the edge of an UHMW−PE film that was used for film thickness determination. On the right, the polymer film can been seen, which ends in folds near the image center followed by the ultraflat mica surface on the left. Bottom: Topographic profile taken from the height image corresponding to the line in the phase image shown above. The average film thickness is 150 ± 30 nm. The arrow indicates the direction of drawing.

Highly Ordered Stacked Lamellae and the Lamellar Doubling. Figure 7 shows an AFM topographic and phase image of an UHMW−PE film surface drawn at 140 °C. The image size is 400 nm × 400 nm. A highly regular crystal morphology can be identified, which is manifested in well stacked lamellae. These lamellae are oriented along the drawing direction into a column of stacked lamellae of 103 ± 12 nm width. The mean lamellar thicknesses for this film are 16.2 ± 2, 29.3 ± 2, and 61.7 ± 2 nm, which indicates an up to twice lamellar doubling (2 × and 4 × 16 nm). Onset and different states of doubling can be clearly seen in the middle crystal stack shown in Figure 7. Amorphous areas separating stacks of crystal chains are up to 30 nm thick, whereas amorphous regions between single-crystal lamellae are less than 15 nm thick. Vertically, height variations between crystalline lamellae and amorphous regions are between 3 ± 1 nm within a single stack. The high degree of order as well as the lamellar doubling is most clearly observed in a sufficiently thin UHMW−PE film. As an AFM line-scan in Figure 8 shows, the film thickness is

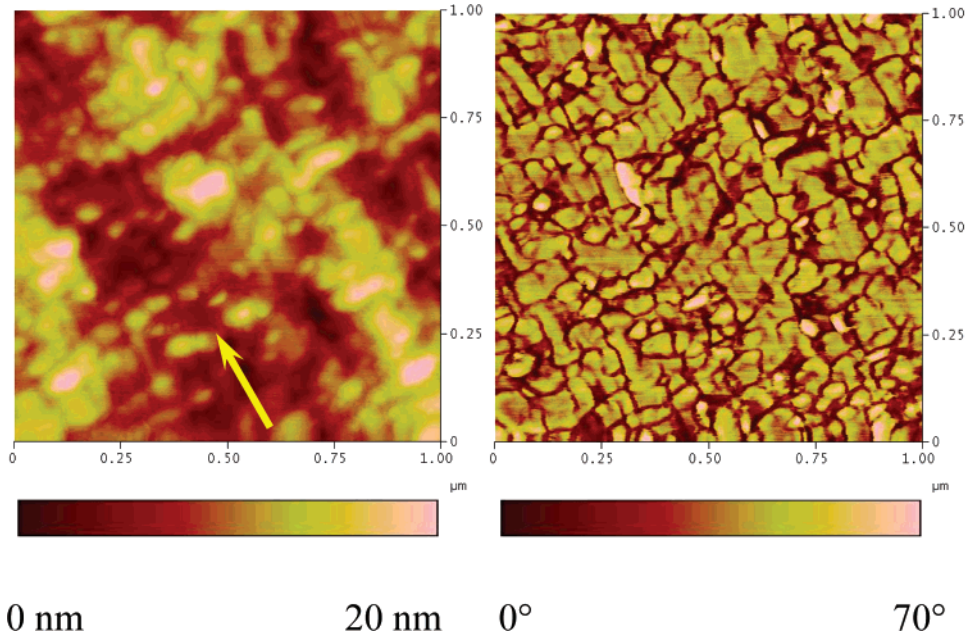

Figure 9. AFM topographic (left) and phase image of an UHMW−PE film annealed at 150 °C. The scan size is 1 μm × 1 μm; the color corresponds to the height and phase change 0−20 nm and 0−70°, respectively. The arrow indicates the drawing direction of the UHMW−PE film.

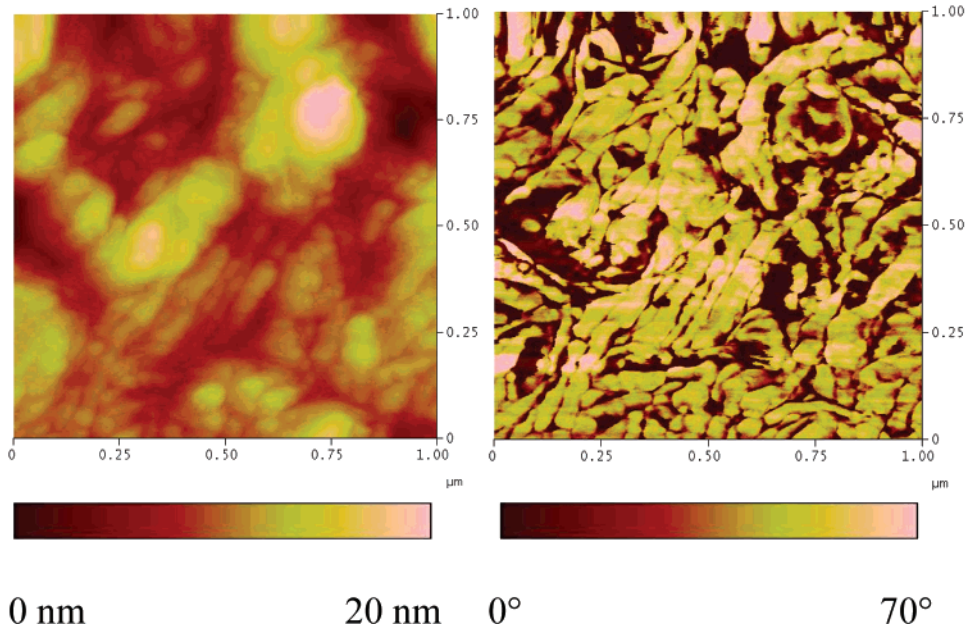

Figure 10. AFM topographic (left) and phase image of an unoriented UHMW−PE film with random orientation. The scan size is 1 μm × 1 μm; the color corresponds to the height and phase change 0−60 nm and 0−70°, respectively.

150 ± 30 nm. Assuming the lamellar width and height to be of the same order, the film consists of a single or at maximum two lamellae across the film thickness. In such thin films the crystalline lamellar stacks develop undisturbed under the applied elongational stress during film drawing and therefore, the high degree of order in the lateral arrangement is induced.

From the results shown in Figure 7, a simple model for the lamellar doubling during the melt drawing process can be proposed.

The models of Dreyfuss and Keller[24] and Rastogi et al.[14] both involve the process of chain sliding during annealing between two adjacent lamellae. Thermodynamically, lamellar crystals tend to reduce the free energy of their fold surfaces by lamellar thickening (diffusional chain sliding).[29] Single chain folds of one lamella are dragged into the adjacent lamella, while increasing their fold length by two. The chains from both lamellae move in opposite directions, finally resulting in a single lamella of double thickness.

During the film drawing, folded chains within a lamellar crystal are subject to the external drawing force. The drawing force is transmitted across the amorphous layer between two stacked lamellae and is therefore believed to be the main factor facilitating the doubling mechanism. A substantial degree of fold regularity is required for the doubling mechanism to occur.[29] In the work discussed here, the regular lamellar stacking of films drawn at 140 °C is introduced during the UHMW−PE melt drawing.

Whereas the model proposed by Rastogi et al.[14] allows for only one doubling of crystalline lamellae, (after doubling the chains get mutually entangled at the doubled crystalline surface)

the model of Barham and Keller,[29] permits a multiple doubling that comprises tripling and quadrupling.

As Figure 7 shows, in the case of ultrathin UHMW−PE melt drawn films only doubling and 2-fold doubling—called quadrupling by Barham and Keller[29]—is observed. Therefore, the current results cannot be fully explained by either of the two models, as more than a single doubling, but no tripling is observed.

This is taken as an indication for a strain-induced lamellar doubling mechanism, which to the best knowledge of the authors is not yet reported up to now. It is believed that the external force is sufficiently high to principally permit multiple doubling. Tripled lamellae are believed to be less stable under an external dragging force, as they arise from originally different thick lamellae, and were therefore not observed in the experiment.

A further indication for a strain induced thickening within melt drawn UHMW−PE films is the fact, that for the UHMW−PE lamellar thickness an upper limit of 25 nm is reported that can be achieved during annealing.[17] Here, a 2-fold quantized thickening is observed with a final thickness of single lamellae of more than 60 nm.

Annealed and Unoriented UHMW—PE Films. To investigate the achievable variety in surface morphology, the films drawn at 140 °C were annealed in vacuum at temperatures of 130, 140, 145, 150, and 160 °C for 12 h. Subsequently, the heating of the oven was switched off and the films were left to cool down to room temperature in vacuum. With increasing annealing temperature, the high degree of anisotropy and the lateral lamellar crystal arrangement was increasingly lost. Figure 9 shows the AFM micrographs of an UHMW−PE film annealed at 150 °C. The drawing direction indicated by the arrow is still visible in the height image, whereas the phase image indicates a slight loss of the original order. Similarly, the rms surface roughness (scan size 1 μm × 1 μm) of the UHMW−PE film drawn at 140 °C increases from 2.4 ± 0.2 nm (see Figure 6) to 3.7 ± 1 nm after annealing for 12 h at 150 °C. As an alternative approach, unoriented films were prepared following the description in the Experimental Section. However, the film was not drawn from the hot glass-plate, but the glass-plate with the polymer film was allowed to cool down before the resulting film was carefully removed. The AFM micrographs in Figure 10 show that the crystal lamellae on the film surface does not exhibit any preferred orientation. As compared to the as drawn films, the significantly higher rms surface roughness of 9 ± 1 nm (scan size 1 μm × 1 μm) of the unoriented film documents the flattening and orientation capabilities of the melt drawing process.

Combining as drawn UHMW−PE films at different temperatures with subsequent annealing treatments and the preparation of unoriented films facilitates a systematical introduction of a surface nanostructure and roughness in the range 1−10 nm range along with different degrees of lateral lamellar order.

Conclusions

In the temperature range from 138 to 146 °C of the UHMW−PE used within this work, crystals and polymer melt coexist in different fractions dependent on the temperature. As a result, ultrathin UHMW−PE films drawn from this two phase state exhibit different lamellar morphologies with different lateral orientations at the film surface and in the bulk as shown by AFM and TEM, respectively. A simple model explaining the observed film morphologies depending on the composition of the two-phase state was presented.

The lamellae in the UHMW−PE ultrathin films drawn at 140 °C show a highly regular stacked arrangement. Lamellar doubling and quadrupling is observed in single-lamella thick UHMW−PE films, which is believed to be mechanical-strain induced.

Acknowledgment. We gratefully acknowledge the partial support from the BMBF for this work within the project Innovations- and Gründerlabor für neue Werkstoffe and Verfahren (IGWV) an der Friedrich-Schiller-Universität Jena, Förderkennzeichen: 03GL0026. We thank Mr. J. Brozek for assistance with the DSC measurement. The authors are grateful to Karin Jandt for proof reading this paper.

References and Notes

(1) Sun, Y. S.; et al. *J. Appl. Polym. Sci.* **2005**, *98*, 474−483.
(2) Kurtz, S. M.; et al. *Biomaterials* **1998**, *19*, 1989−2003.
(3) Taddei, P.; Affatato, S.; Fagnano, C.; Toni, A. *Biomacromolecules* **2006**, *7*, 1912−1920.
(4) Heuberger, M. P.; Widmer, M. R.; Zobeley, E.; Glockshuber, R.; Spencer, N. D. *Biomaterials* **2005**, *26*, 1165−1173.
(5) Rezaei, M.; Ebrahimi, N. G.; Kontopoulou, M. *J. Appl. Polym. Sci.* **2006**, *99*, 2344−2351.
(6) Petermann, J.; Gohil, R. M. *J. Mater. Sci.* **1979**, *14*, 2260−2264.
(7) Schultz, J. M.; Petermann, J. *Colloid Polym. Sci.* **1984**, *262*, 294−300.
(8) Petermann, J.; Schultz, J. M. *Colloid Polym. Sci.* **1984**, *262*, 217−222.
(9) Fuchs, H.; et al. *Polym. Bull. (Berlin)* **1991**, *26*, 95−100.
(10) Jandt, K. D.; Eng, L. M.; Petermann, J.; Fuchs, H. *Polymer* **1992**, *33*, 5331−5333.
(11) Jandt, K. D.; Buhk, M.; Miles, M. J.; Petermann, J. *Polymer* **1994**, *35*, 2458−2462.
(12) Jandt, K. D.; Mc Master, J.; Miles, M. J.; Petermann, J. *Macromolecules* **1993**, *26*, 6552−6556.
(13) Zhao, Y.; Zhang, W. G.; Yang, D. C. *J. Mater. Sci. Lett.* **1993**, *12*, 1309−1312.
(14) Rastogi, S.; Spoelstra, A.; Goossens, J. G. P.; Lemstra, P. J. *Macromolecules* **1997**, *30*, 7880−7889.
(15) Bershtein, V. A.; Egorov, V. M.; Kemp, T. J. *Differential Scanning Calorimetry of Polymers*; Ellis Horwood Ltd.: Chichester, U.K., 1994.
(16) Zhang, J.; et al. *Macromolecules* **2002**, *35*, 8869−8877.
(17) Rastogi, S.; et al. *Nat. Mater.* **2005**, *4*, 635−641.
(18) Keller, A. Introductory lecture—Aspects of polymer gels. *Faraday Discuss.* **1995**, 1−49.
(19) Jian, T.; Shyu, W.; Lin, W.; Chen, K.; Yeh, J. T. *Polym. Eng. Sci.* **2003**, *43*, 1765−1777.
(20) Jandt, K. D. *Surf. Sci.* **2001**, *491*, 303−332.
(21) Zhang, B.; Zhao, Y.; Yang, D.; Wang, E. K. *J. Mater. Sci. Lett.* **1995**, *14*, 1275−1277.
(22) Jandt, K. D.; Buhk, M.; Petermann, J.; Eng, M. L.; Fuchs, H. *Polym. Bull. (Berlin)* **1991**, *27*, 101−107.
(23) Li, Y.; Goddard, W. A. *Macromolecules* **2002**, *35*, 8440−8455.
(24) Dreyfuss, P.; Keller, A. *J. Macromol. Sci. Phys.* **1970**, *B4*, 811.
(25) Mehling, R. 2003, Dissertation, University of Stuttgart, Germany.
(26) Kwon, Y. K.; Boller, A.; Pyda, M.; Wunderlich, B. *Polymer* **2000**, *41*, 6237−6249.
(27) Han, C. D. *Rheology in Polymer Processing*; Academic Press: New York 1976.
(28) Smook, J.; Pennings, A. J. *J. Mater. Sci.* **1984**, *19*, 31−43.
(29) Barham, P. J.; Keller, A. J. *J. Polym. Sci., Part B: Polym. Phys.* **1989**, *27*, 1029−1042.

MA070613X